










## Discovery of a millisecond pulsar associated with Terzan 6

SHI-JIE GAO <sup>1,2</sup> YI-XUAN SHAO <sup>1,2</sup> PEI WANG <sup>3,4</sup> PING ZHOU <sup>1,2</sup> XIANG-DONG LI <sup>1,2</sup> LEI ZHANG <sup>3,5</sup>  
JOSEPH W. KANIA <sup>6,7</sup> DUNCAN R. LORIMER <sup>6,7</sup> AND DI LI <sup>8,3</sup>

<sup>1</sup>*School of Astronomy and Space Science, Nanjing University, Nanjing, 210023, People's Republic of China*

<sup>2</sup>*Key Laboratory of Modern Astronomy and Astrophysics, Nanjing University, Ministry of Education, Nanjing, 210023, People's Republic of China*

<sup>3</sup>*National Astronomical Observatories, Chinese Academy of Sciences, Beijing, People's Republic of China*

<sup>4</sup>*Institute for Frontiers in Astronomy and Astrophysics, Beijing Normal University, Beijing 102206, People's Republic of China*

<sup>5</sup>*CSIRO Astronomy and Space Science, P.O. Box 76, Epping, NSW 1710, Australia*

<sup>6</sup>*Center for Gravitational Waves and Cosmology, West Virginia University, Chestnut Ridge Research Building, Morgantown, WV, USA*

<sup>7</sup>*Department of Physics and Astronomy, West Virginia University, Morgantown, WV, USA*

<sup>8</sup>*Department of Astronomy, Tsinghua University, Beijing 100084, People's Republic of China*

### ABSTRACT

Observations show that globular clusters might be among the best places to find millisecond pulsars. However, the globular cluster Terzan 6 seems to be an exception without any pulsar discovered, although its high stellar encounter rate suggests that it harbors dozens of them. We report the discovery of the first radio pulsar, PSR J1750–3116A, likely associated with Terzan 6 in a search of C-band (4–8 GHz) data from the Robert C. Byrd Green Bank Telescope with a spin period of 5.33 ms and dispersion measure,  $DM \simeq 383 \text{ pc cm}^{-3}$ . The mean flux density of this pulsar is approximately  $3 \mu\text{Jy}$ . The DM agrees well with predictions from the Galactic free electron density model, assuming a distance of 6.7 kpc for Terzan 6. PSR J1750–3116A is likely an isolated millisecond pulsar, potentially formed through dynamical interactions, considering the core-collapsed classification and the exceptionally high stellar encounter rate of Terzan 6. This is the highest radio frequency observation that has led to the discovery of a pulsar in a globular cluster to date. While L-band (1–2 GHz) observations of this cluster are unlikely to yield significant returns due to propagation effects, we predict that further pulsar discoveries in Terzan 6 will be made by existing radio telescopes at higher frequencies.

*Keywords:* Millisecond pulsars (1062) — Globular star clusters (656) — Neutron stars (1108)

### 1. INTRODUCTION

Globular clusters (GCs) are gravitationally bound star clusters characterized by relatively high stellar densities toward their centers (Gratton et al. 2019). The dense environment facilitates a high birth rate of low-mass X-ray binaries (LMXBs), which are the progenitors of millisecond pulsars (MSPs; see, for example, Ivanova 2013). Consequently, GCs are ideal places for searching for pulsars compared to the Galactic disk. Currently, there are 330 pulsars known to be associated with GCs (see Paulo Friere's catalog of Pulsars in Globular clusters<sup>1</sup>

for more details). While most of them are MSPs, which are expected given the age of GCs and their high specific incidence of LMXB, there are also several anomalous younger long-period ( $\gtrsim 1 \text{ s}$ ) pulsars discovered in old GCs (Lyne et al. 1996; Boyles et al. 2011; Zhou et al. 2024; Wu et al. 2023).

Terzan 6 is a metal-rich core-collapsed Galactic GC (Trager et al. 1995; Barbuy et al. 1997) centered at  $\alpha_{J2000} = 17^{\text{h}}50^{\text{m}}46^{\text{s}}.854$ ,  $\delta_{J2000} = -31^{\circ}16'29''.384$  (in *T* Zand et al. 2003). Optical and near-infrared photometric observations indicate the distance to Terzan 6 to be 6.7 kpc (Fahlman et al. 1995; Barbuy et al. 1997; Valenti et al. 2007). Figure 1 shows the Ks-band image of Terzan 6 (Minniti 2018). The core and half-light radii (green circle in Figure 1) of Terzan 6 are  $3''$  and  $0''.4$ , respectively (Harris 1996). Located in the direction of the

Corresponding author: Shi-Jie Gao & Xiang-Dong Li  
gaosj@smail.nju.edu.cn, lixd@nju.edu.cn

<sup>1</sup> <https://www3.mpifr-bonn.mpg.de/staff/pfriere/GCpsr.html>

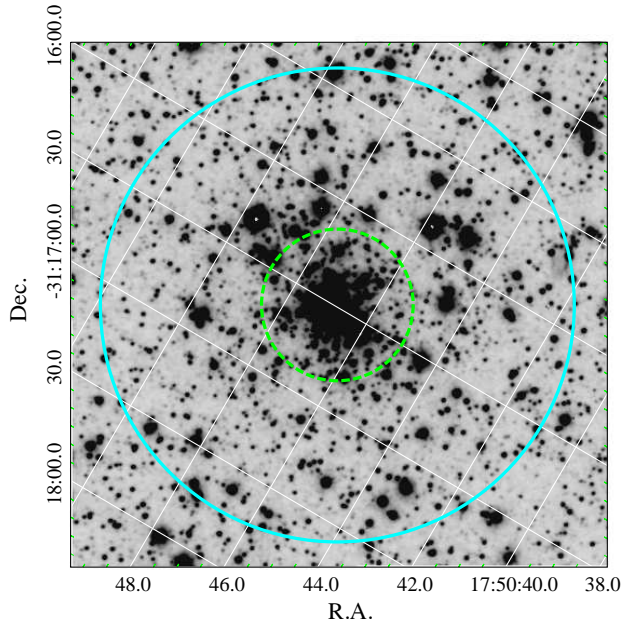


**Figure 1.** Ks-band image of Terzan 6 (Minniti 2018). The green circle represents the half-light radius ( $0.4'$ ) of Terzan 6, and the cyan circle the beam size ( $2.5'$ , full-width at half-maximum) of the GBT’s C-band receiver.

Galactic bulge, Terzan 6 is  $2.2'$  below the Galactic plane with a high extinction  $E(B - V) = 2.35$  (Valenti et al. 2007).

The stellar encounter rate  $\Gamma \propto \rho_0^{1.5} r_c$  (where  $\rho_0$  is the central mass density and  $r_c$  is the core radius) is an important indicator for characterizing the dynamics of GCs. It is well known that  $\Gamma$  correlates with the number of pulsars within a GC (Pooley et al. 2003; Abdo et al. 2009), and the expected number  $\lambda$  of potential radio pulsars could be estimated from the following relation suggested by Turk & Lorimer (2013):  $\ln \lambda = -1.1 + 1.5 \log \Gamma$ . Table 1 summarizes the measured and inferred parameters of some Galactic GCs with high  $\Gamma$  values. Here the  $\Gamma$  values are normalized such that 47 Tuc has  $\Gamma = 1000$  (Bahramian et al. 2013). Terzan 6 is among the GCs with highest  $\Gamma$  values, placing it as a favorable host of LMXBs, MSPs, and merger/accretion-induced collapse products (e.g., Verbunt & Hut 1987; Pooley et al. 2003; Verbunt & Freire 2014; Kremer et al. 2021, 2022, 2023; Ye et al. 2024). According to the  $\lambda - \Gamma$  relation, Terzan 6 is expected to harbor around 54 radio pulsars. GCs with similar  $\Gamma$  values with Terzan 6 such as Terzan 5 (Padmanabh et al. 2024), M15 (Wu et al. 2023) and NGC 6441<sup>2</sup>, have 49, 14 and 9 confirmed pulsars, respectively. Although two

<sup>2</sup> <https://trapum.org/discoveries/>

X-ray sources have been indeed identified in Terzan 6, i.e., the transient LMXB GRS 1747–312 (Predehl et al. 1991) and the eclipsing LMXB burster Terzan 6 X2 (van den Berg et al. 2024), no MSPs have been detected so far. A similar situation occurs in NGC 6715, probably due to its very large distance of 26.5 kpc, while Terzan 6 is the second nearest GC listed in Table 1.

Here we report the discovery a 5.33 ms pulsar associated with Terzan 6, referred to as PSR J1750–3116A. The rest of this letter is structured as follows. We describe the observations and data reduction processes in section 2. The search results are presented in section 3. We discuss the implications of these results in section 4. Our conclusions are provided in section 5.

## 2. OBSERVATIONS AND DATA REDUCTION

Observations of Terzan 6 were conducted with the Robert C. Byrd Green Bank Telescope (GBT; Prestage et al. 2009) using the C-band receiver on two occasions: MJD 58625 (UTC 2019-05-22) and MJD 58626 (UTC 2019-05-23) (project ID: AGBT19A\_477, PI: Duncan Lorimer). The beam size (full-width at half-maximum) of the C-band receiver is  $2.5^{\circ}$  (cyan circle in Figure 1)<sup>3</sup>, providing a good coverage of Terzan 6. Data were recorded with 3072 frequency channels covering a total effective bandwidth 3.8 GHz centered at 6 GHz. The time resolution was  $87.381 \mu\text{s}$  and the integration time for both observations was  $\sim 4.6$  hours. The system temperature of the GBT’s C-band receiver increased by several K at the beginning and end of  $\sim 0.5$  hour of the observations, likely due to atmospheric opacity when Terzan 6 (Decl.  $\sim -31^{\circ}$ ) was visible at low elevations. Consequently, the first and last  $\sim 500 - 2000$  s observational data were excluded in the following analysis.

We searched for periodic dispersed pulsations using the Pulsar Exploration and Search TOolkit<sup>4</sup> (PRESTO, Ransom 2011). We first used the PRESTO routine `rfifind` to mask and zap radio-frequency interference (RFI) in both the time and frequency domains. Then the search-mode PSRFITS-format<sup>5</sup> data were de-dispersed with the PRESTO routine `prepsubband`<sup>6</sup> to form barycentric time-series in a dispersion measure (DM) range of  $0 - 1000 \text{ pc cm}^{-3}$ , with a step of  $0.5 \text{ pc cm}^{-3}$ , following the PRESTO Python script `DDplan.py`. Subsequently, the PRESTO routine

<sup>3</sup> <https://www.gb.nrao.edu/scienceDocs/GBTpg.pdf>

<sup>4</sup> <https://github.com/scottransom/presto>

<sup>5</sup> [https://www.atnf.csiro.au/research/pulsar/psrfits\\_definition/Psrfits.html](https://www.atnf.csiro.au/research/pulsar/psrfits_definition/Psrfits.html)

<sup>6</sup> Utilizing a GPU-version ([https://github.com/zdj649150499/Presto\\_GPU](https://github.com/zdj649150499/Presto_GPU)) running on a NVIDIA<sup>®</sup> A100 GPU.

**Table 1.** GCs with the highest  $\Gamma$  values, providing their distances  $d$  (Harris 1996),  $\Gamma$  values (Bahramian et al. 2013), the number  $N_{\text{psr}}$  of known pulsars, the number of known isolated pulsars  $N_{\text{iso}}$  and the expected number  $\lambda$  of potential radio pulsars.

| GCs <sup>a</sup>             | $d$ (kpc) | $\Gamma$ <sup>b</sup> | $N_{\text{psr}}$ <sup>c</sup> | $N_{\text{iso}}$ <sup>c</sup> | $\lambda$ <sup>d</sup> |
|------------------------------|-----------|-----------------------|-------------------------------|-------------------------------|------------------------|
| Terzan 5                     | 6.9       | 6800                  | 49                            | 20                            | 104                    |
| *NGC 7078 (M 15)             | 10.4      | 4510                  | 14                            | 13                            | 80                     |
| NGC 6715 (M 54)              | 26.5      | 2520                  | 0                             | 0                             | 55                     |
| *Terzan 6                    | 6.7       | 2470                  | 0                             | 0                             | 54                     |
| NGC 6441                     | 11.6      | 2300                  | 9                             | 6                             | 52                     |
| *NGC 6266 (M62) <sup>e</sup> | 6.8       | 1670                  | 10                            | 0                             | 42                     |
| NGC 1851                     | 12.1      | 1530                  | 15                            | 6                             | 40                     |
| NGC 6440                     | 8.5       | 1400                  | 8                             | 4                             | 37                     |
| *NGC 6624                    | 7.9       | 1150                  | 12                            | 10                            | 33                     |
| *NGC 6681 (M 70)             | 9.0       | 1040                  | 3                             | 2                             | 31                     |
| NGC 104 (47 Tuc)             | 4.5       | 1000                  | 36                            | 12                            | 30                     |

NOTE—<sup>a</sup> Core-collapsed GCs are indicated by “\*” (Harris 1996). <sup>b</sup>  $\Gamma$  values are normalized to give 47 Tuc’s  $\Gamma = 1000$ . <sup>c</sup> Numbers of known pulsars are referred to Paulo Friere’s catalog<sup>1</sup>. <sup>d</sup>  $\ln \lambda = -1.1 + 1.5 \log \Gamma$  (Turk & Lorimer 2013). <sup>e</sup> NGC 6266 is either core-collapsed or on the verge of collapsing, see discussion in Vleschow et al. (2024).

`accelsearch` was employed to search for periodic signals with a Fourier-domain acceleration search technique (Ransom et al. 2002). The summed number of harmonics was up to 16 and the maximum Fourier frequency derivative to search was set to  $\mathbf{zmax} = \dot{f}T_{\text{obs}}^2 = 100$ , where  $\dot{f}$  and  $T_{\text{obs}}$  are the spin frequency derivative and the total observation length, respectively. This corresponds to a maximum drift of the physical linear acceleration  $a = c\dot{f}/f = \mathbf{zmax} \times c/(fT_{\text{obs}}^2)$ , where  $c$  is the speed of light in vacuum and  $f$  is the spin frequency. Candidates generated by `accelsearch` were winnowed using the Python script `ACCEL_sift.py` of PRESTO with a sigma threshold greater than 4.0. Finally, the folded diagnostic plots were produced by the PRESTO routine `prepfold` and were inspected by eye to identify the promising candidates.

### 3. RESULTS

We found a faint pulsar candidate PSR J1750–3116A with a spin period  $P \simeq 5.33$  ms and DM  $\simeq 383$  pc cm<sup>-3</sup> in the second observation on MJD 58626. Figure 2 shows the folding results generated by the PRESTO routine `prepfold`. The significance of the detection is computed by calculating the reduced- $\chi^2$  statistic for a model assuming no pulsations (Leahy et al. 1983). The reduced- $\chi^2$  is 3.230 with an effective degrees of freedom of 39.25 (for details, see Appendix E of Bachetti et al. 2021). The probability that the signal might be due to noise is  $< 3.81 \times 10^{-11}$ , which is expressed in terms of equivalent Gaussian significance of 6.5- $\sigma$ . The lower-left and upper-middle panels show the phase vs. time and phase vs. observing frequency relations, respectively, where the pulsar features (two vertical lines) can be easily identified. The cumulative profile is plotted on the

top of the left panel. The sidebar at the right of the left panel shows the increase in the reduced- $\chi^2$  with the observing time. The lower-middle panel illustrates the dispersion measure vs. reduced- $\chi^2$ , with a peak located at  $\simeq 383.08$  pc cm<sup>-3</sup>. The right panels show the reduced- $\chi^2$  with respect to period and period derivative, where the highest values of reduced- $\chi^2$  indicate the best-fit of the observed period and period derivative.

We failed to detect the 5.33 ms signal during a blind search of the first observation on MJD 58625. Using the folding results of the second observation, however, we successfully folded the data with the same DM and  $P$  during the first observation, which is shown in Figure 3. Although the signal in the first observation is much weaker than on MJD 58626, when folded using the parameters found above, the pulsar-like features are clearly discernible. The dimming in the first observation may be due to scintillation or intrinsic emission variations of the pulsar.

Neither significant acceleration (the PRESTO routine `accelsearch` gives  $-0.00185(93)$  ms<sup>-2</sup> for the first observation) nor barycentric period variation between the two observations was detected, suggesting that the pulsar is either isolated or in a long-period orbit. An isolated pulsar seems to be consistent with the Terzan 6’s classification as a core-collapsed cluster, where dynamical interaction processes are more frequent and intense. Isolated MSPs could be formed from neutron star–main-sequence star tidal disruption events (Kremer et al. 2022; Ye et al. 2024), gravitational collapse of double white dwarf merger remnants (Ye et al. 2024), and disruption of MSP binaries by dynamical interactions during core collapse of the cluster (Verbunt & Freire 2014). As shown in Table 1, core-collapsed GCs generally have

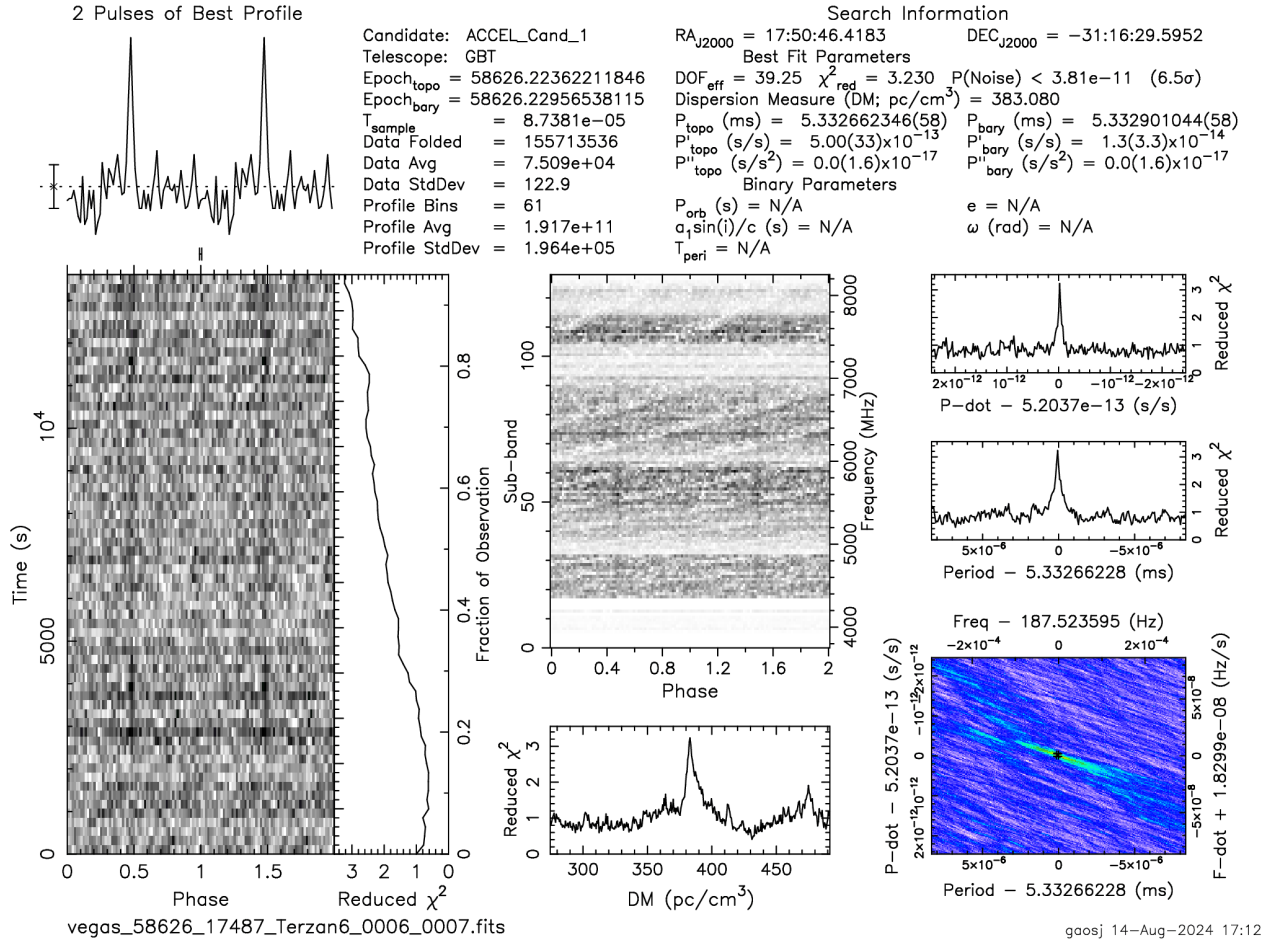


**Figure 2.** Discovery plot of PSR J1750–3116A from the second observation on MJD 58626, generated by PRESTO routine `prepfold`. The lower-left and upper-middle panels show the phase vs. time and phase vs. observing frequency, respectively. The cumulative profile is plotted at the top of the left panel and the sidebar to the right of the left panel shows the increase in the reduced- $\chi^2$  (reflecting the increased level of statistical significance) with observing time. The lower-middle panel shows the reduced- $\chi^2$  vs. dispersion measure, with a peak located at DM = 383.08 pc cm<sup>-3</sup>. The right panels show the reduced- $\chi^2$  respect to trial period and period derivative, where the highest values of reduced- $\chi^2$  indicate the best-fit of observed period and period derivative.

high ratios of  $N_{\text{iso}}/N_{\text{psr}}$ , e.g., 13/14 for NGC 7078 (M15) and 10/12 for NGC 6624. Whether PSR J1750–3116A is isolated needs to be confirmed or falsified by further follow-up observations. Nevertheless, assuming that the pulsar is isolated, we tried to obtain the spin frequency through connecting the two observations. We used the PRESTO Python scripts `pygaussfit.py` and `get_TOAs.py` to form a standard reference template profile and extracted the times of arrival (TOAs) of these two observations, respectively. We also fixed the location of PSR J1750–3116A according to the pointing of the beam of the second observation and DM. Using

TEMPO2<sup>7</sup> (Nice et al. 2015) the spin frequency was fitted to be 187.515196274(72) Hz. The input and output parameters are summarized in Table 2.

#### 4. DISCUSSION

The high DM of 383 pc cm<sup>-3</sup> for PSR J1750–3116A places Terzan 6 as the GC with the second highest DM to date behind GLIMPSE-C01 (with DM  $\sim$  450 – 520 pc cm<sup>-3</sup>; McCarver et al. 2024). Adopting a distance of 6.7 kpc to Terzan 6, the Galactic electron density models YMW2016 (Yao et al. 2017)

<sup>7</sup> <https://sourceforge.net/projects/tempo2>



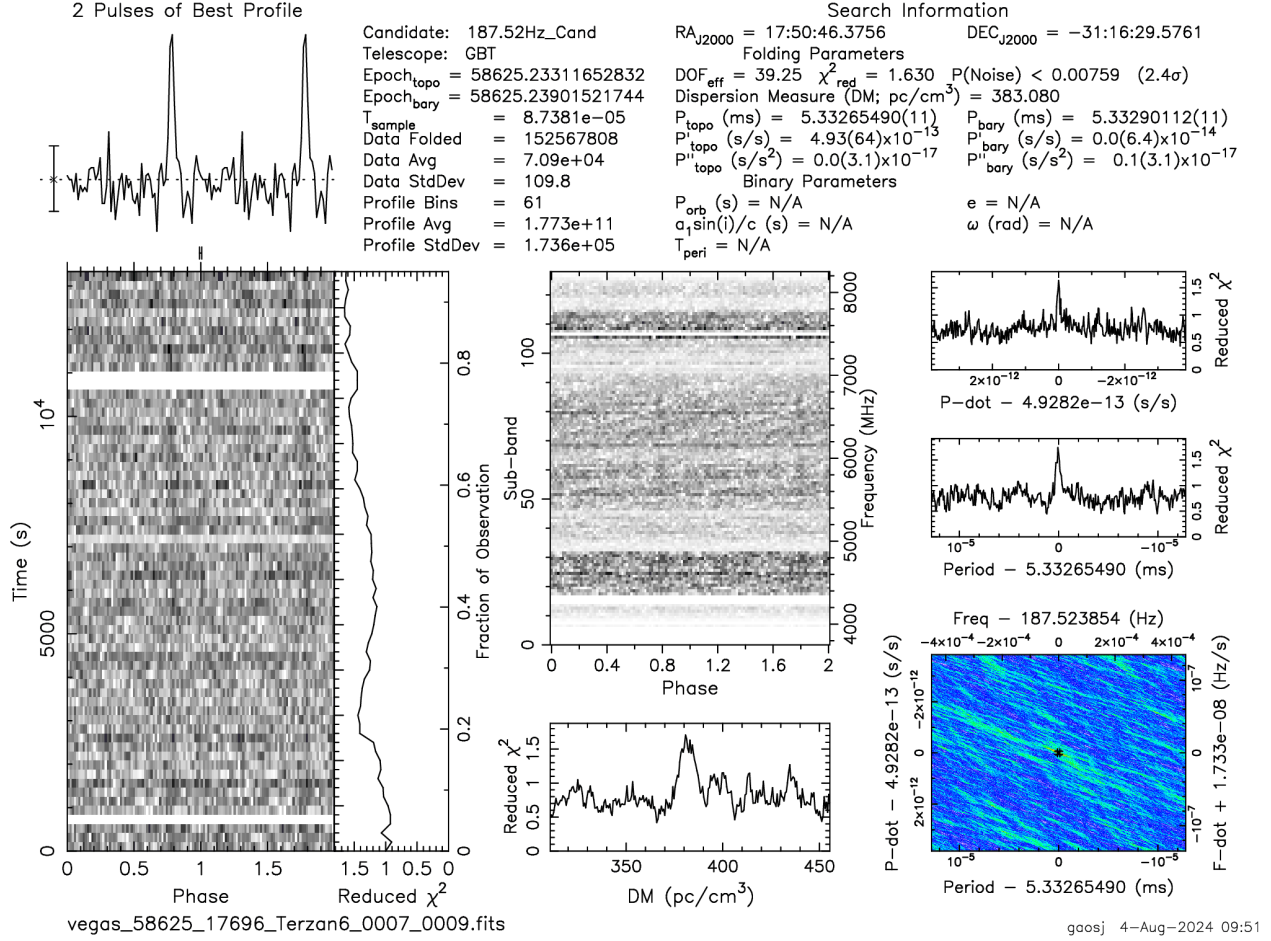


Figure 3. Similar to Figure 2 but for the first observation on MJD 58625.

Table 2. TEMPO2’s input and output parameters for PSR J1750–3116A.

| PSR                       |         | J1750–3116A                 |
|---------------------------|---------|-----------------------------|
| R.A. (J2000, hh:mm:ss)    | fixed   | 17:50:46(11.7) <sup>a</sup> |
| Decl. (J2000, dd:mm)      | fixed   | –31:16(2.5) <sup>a</sup>    |
| Dispersion measure        | fixed   | 383.08 pc cm <sup>–3</sup>  |
| Spin frequency derivative | fixed   | 0.0                         |
| Spin frequency            | fitted  | 187.515196274(72) Hz        |
| Spin period               | derived | 0.0053329011188(20) s       |
| Timing epoch              | ...     | MJD 58626                   |
| Total time span           | ...     | 1.128 d                     |
| Number of TOAs            | ...     | 13                          |
| Post-fit residual         | ...     | 48.495 $\mu$ s              |

NOTE—<sup>a</sup> The uncertainties for the position are set to the beam size (2.5′) of the GBT’s C-band receiver. During fitting, the position is set to the center coordinates (R.A., Decl.) = (17<sup>h</sup>50<sup>m</sup>46<sup>s</sup>.42, –31°16′30″.00), which is where the GBT’s C-band receiver was pointed during the second observation.

and NE2001 (Cordes & Lazio 2002) predict the DM values to be  $271 \text{ pc cm}^{-3}$  and  $397 \text{ pc cm}^{-3}$ , respectively<sup>8</sup>. The measured DM for PSR J1750–3116A falls between them, strongly supporting the association between PSR J1750–3116A and Terzan 6.

We now discuss the potential detectability of pulsars in Terzan 6 based on our searching results. The flux density of PSR J1750–3116A can be estimated from the signal-to-noise ratio and the off-pulse noise (see, e.g., Lorimer & Kramer 2004). The root-mean-square (RMS) variations in the system noise

$$\Delta S_{\text{sys}} = \frac{T_{\text{sys}}}{G\sqrt{n_p t_{\text{bin}} \Delta\nu}} = C\sigma_p, \quad (1)$$

where  $T_{\text{sys}} = 21.3 \text{ K}$  is the total system temperature,  $G = 2.0 \text{ K Jy}^{-1}$  is the telescope gain,  $n_p = 2$  is the number of summed polarizations,  $t_{\text{bin}}$  is the observation time per phase bin,  $\Delta\nu$  is the effective bandwidth (2250 MHz after RFI zapping). As shown in this expression, these quantities are related to the off-pulse RMS,  $\sigma_p$ , by the scaling factor  $C$ . From an uncalibrated pulse profile from which we measure  $\sigma_p$ , this expression allows us to compute the scaling factor from which a mean flux density can be readily calculated by integrating the scaled pulse profile. Using this approach, we find a mean flux density of  $3.8 \mu\text{Jy}$  for the discovery observation (Figure 2, where  $t_{\text{bin}} = 223 \text{ s}$ ) and  $2.1 \mu\text{Jy}$  for the confirmation observation (Figure 3, where  $t_{\text{bin}} = 218 \text{ s}$ ). It should be noted that this approach is only valid when the off-pulse noise is Gaussian-like. However, as shown in the phase vs. time and phase vs. observing frequency panels in Figure 2 and Figure 3, some RFI in both time and observing frequency domains remains present in the otherwise Gaussian-like off-pulse regions, indicating that the flux density is somewhat underestimated and should be treated as a lower limit.

Pulsars typically have a negative spectral index (around  $-1.4$ , Bates et al. 2013), implying that their flux densities are higher at lower frequencies. Adopting an index of  $-1.4$ , we estimate the flux density of PSR J1750–3116A at L-band  $S_{1.4 \text{ GHz}} \sim 23 \mu\text{Jy}$ , suggesting that the pulsar may be bright enough to be detected with the L-band receivers of GBT (which has a  $10\text{-}\sigma$  sensitivity limit  $\sim 13.2 \mu\text{Jy}$  for a 4-hour integration at 1.44 GHz<sup>9</sup>) or MeerKAT (which has  $10\text{-}\sigma$  sensitivity limit  $\sim 13 \mu\text{Jy}$  for a 2.5-hour integration at 1.3 GHz, Ridolfi et al. 2021). Since observations at higher fre-

quencies tend to detect pulsars with flatter spectra, the spectral index may be flatter than  $-1.4$  for a typical pulsar. Therefore, the estimated flux density at L-band should be considered as an upper limit. Even worse, significant scatter broadening and smearing due to the high dispersion measure might prohibit detection, especially for fastest MSPs (spin period  $< 10 \text{ ms}$ ; Ridolfi et al. 2021). Additionally, since Terzan 6 is only  $\sim 2$  away from the Galactic center, the sky temperatures at 1.4 GHz (L-band), 2.0 GHz (S-band) and 6 GHz (C-band) are 11.5 K, 6.4 K and 3.0 K for Terzan 6, respectively<sup>10</sup>. This extra contribution to the telescope’s system temperature  $T_{\text{sys}}$  further complicates possible pulsar detection in L or S-band. These factors may explain why Lynch et al. (2011) did not detect any pulsars in Terzan 6 during a 2-hour observation with the GBT S-band (centered at 2 GHz) receiver. Our C-band detection of PSR J1750–3116A makes it possible for further follow-up L or S-band observations which make use of the now known DM. This may lead to new detections of pulsars in Terzan 6.

To estimate how many MSPs might be detectable in the future, we can take the predicted number from Turk & Lorimer (2013) given in Table 1 for Terzan 6, i.e.  $\lambda = 54$ . Assuming a log-normal luminosity function (see, e.g., Faucher-Giguère & Kaspi 2006), above some limiting luminosity,  $L_{\text{min}}$ , the expected number of detectable pulsars

$$N_{\text{det}} \simeq \frac{\lambda}{2} \times \text{erfc} \left[ \frac{\log L_{\text{min}} - \mu^0}{\sqrt{2}\sigma^0} \right], \quad (2)$$

where  $\mu^0$  and  $\sigma^0$  are, respectively, the mean and standard deviation of the log-normal luminosity function. For a reference observing frequency of 1.4 GHz, we take the standard values of these parameters  $\mu^0 = -1.1$  and  $\sigma^0 = 0.9$  that are consistent with GC populations (Bagchi et al. 2011). The scaled 1.4 GHz flux density of  $23 \mu\text{Jy}$  derived above for PSR J1750–3116A corresponds to a luminosity of around  $1.0 \text{ mJy kpc}^2$ . Setting this to be the value of  $L_{\text{min}}$  in Equation 2, leads to an expected number of around 6 MSPs above this limit. Further and deeper searches of Terzan 6 are indeed warranted.

## 5. CONCLUSIONS

We report the discovery of the 5.33 ms pulsar J1750–3116A in a targeted search of Terzan 6 with the GBT at C-band (4–8 GHz). This is the highest frequency discovery observation for a GC search to date. The pulsar has a dispersion measure of  $\sim 383 \text{ pc cm}^{-3}$ , which is

<sup>8</sup> Calculated using PyGEDM (Price et al. 2021) web app (<https://apps.datacentral.org.au/pygedm/>).

<sup>9</sup> Estimated by the GBT Sensitivity Calculator ([https://dss.gb.nrao.edu/calculator-ui/war/Calculator\\_ui.html](https://dss.gb.nrao.edu/calculator-ui/war/Calculator_ui.html)).

<sup>10</sup> Calculated using PyGDSM (Price 2016). The temperatures include a 2.725 K contribution from the cosmic microwave background.

the second highest DM value among all GCs containing radio pulsars. The DM is compatible with that predicted by the Galactic free electron density model NE2001 (Cordes & Lazio 2002), provided that Terzan 6 is 6.7 kpc away. PSR J1750–3116A is probably isolated, consistent with the Terzan 6’s classification as a core-collapsed cluster, where dynamical interaction processes are more frequent and intense. These two factors lend support to the suggestion that the pulsar is associated with Terzan 6. The discovery of other pulsars with the same DM value of PSR J1750–3116A would provide definitive evidence of the association between PSR J1750–3116A and Terzan 6.

We estimate the flux density of PSR J1750–3116A to be  $\sim 3 \mu\text{Jy}$  at 6 GHz. Assuming a spectral index of  $-1.4$ , the flux density at 1.44 GHz is inferred to be  $23 \mu\text{Jy}$ , which is above the sensitivity limits for the GBT and MeerKAT L-band receivers. In consideration of the exceptionally high stellar encounter rate, more sensitive searches such as using GBT and MeerKAT (e.g., TRAPUM, a MeerKAT large survey project, Stappers & Kramer 2016) are expected to result in further pulsar discoveries in Terzan 6. The more sensitive and long-term high-cadence follow-up observations can provide a phase-connected timing solution for PSR J1750–3116A and hence localize its position to cross-check with the X-ray and  $\gamma$ -ray data.

#### ACKNOWLEDGEMENTS

We are grateful to the anonymous referee for their careful reading and insightful comments. S.J.G. would like to thank Evan Smith and Brenne Gregory for their assistance in transferring GBT archival data, Yang Chen and Yi-Wei Bao for providing the NVIDIA A100 GPU and De-Jiang Zhou for help with installing and using of the GPU-version PRESTO. The National Radio Astronomy Observatory is a facility of the National Science Foundation operated under cooperative agreement by Associated Universities, Inc. The Green Bank Observatory is a facility of the National Science Founda-

tion operated under cooperative agreement by Associated Universities, Inc. S.J.G. acknowledges support from the National Natural Science Foundation of China (NSFC) under grant No. 123B2045. X.D.L. acknowledges support from the National Key Research and Development Program of China (2021YFA0718500), the National Natural Science Foundation of China (NSFC) under grant No. 12041301, 12121003 and 12203051. P.W. acknowledges support from the National Natural Science Foundation of China (NSFC) Programs No. 11988101, 12041303, the CAS Youth Interdisciplinary Team, the Youth Innovation Promotion Association CAS (id. 2021055), and the Cultivation Project for FAST Scientific Payoff and Research Achievement of CAMS-CAS. P.Z. acknowledges support from the National Natural Science Foundation of China (NSFC) under grant No. 12273010. L.Z. is supported by the National Natural Science Foundation of China (NSFC) under grant No. 12103069. Di Li is a New Cornerstone investigator. The computation was made by using the facilities at the High-Performance Computing Center of Collaborative Innovation Center of Advanced Microstructures (Nanjing University).

#### DATA AVAILABILITY

Raw PSRFITS format data can be accessed through the [NRAO Archive Interface](#) by contacting the GBT staff with project ID: AGBT19A\_477. Ks-band image of Terzan 6 are based on data obtained from the ESO Science Archive Facility with DOI: [10.18727/archive/68](#). Reduced data are available on the ScienceDB platform with DOI: [10.57760/sciencedb.12966](#).

*Facilities:* The Green Bank Observatory Robert C. Byrd Green Bank Telescope (Prestage et al. 2009).

*Software:* PRESTO (Ransom 2011), TEMPO2 (Nice et al. 2015), DS9 (Joye & Mandel 2003), PyGEDM (Price et al. 2021) and PyGDSM (Price 2016).

#### REFERENCES

- Abdo, A. A., Ackermann, M., Ajello, M., et al. 2009, *Science*, 325, 848, doi: [10.1126/science.1176113](#)
- Bachetti, M., Pilia, M., Huppenkothen, D., et al. 2021, *ApJ*, 909, 33, doi: [10.3847/1538-4357/abda4a](#)
- Bagchi, M., Lorimer, D. R., & Chennamangalam, J. 2011, *MNRAS*, 418, 477, doi: [10.1111/j.1365-2966.2011.19498.x](#)
- Bahramian, A., Heinke, C. O., Sivakoff, G. R., & Gladstone, J. C. 2013, *ApJ*, 766, 136, doi: [10.1088/0004-637X/766/2/136](#)
- Barbuy, B., Ortolani, S., & Bica, E. 1997, *A&AS*, 122, 483, doi: [10.1051/aas:1997148](#)
- Bates, S. D., Lorimer, D. R., & Verbiest, J. P. W. 2013, *MNRAS*, 431, 1352, doi: [10.1093/mnras/stt257](#)
- Boyles, J., Lorimer, D. R., Turk, P. J., et al. 2011, *ApJ*, 742, 51, doi: [10.1088/0004-637X/742/1/51](#)
- Cordes, J. M., & Lazio, T. J. W. 2002, arXiv e-prints, astro, doi: [10.48550/arXiv.astro-ph/0207156](#)

- Fahlman, G. G., Douglas, K. A., & Thompson, I. B. 1995, *AJ*, 110, 2189, doi: [10.1086/117678](https://doi.org/10.1086/117678)
- Faucher-Giguère, C.-A., & Kaspi, V. M. 2006, *ApJ*, 643, 332, doi: [10.1086/501516](https://doi.org/10.1086/501516)
- Gratton, R., Bragaglia, A., Carretta, E., et al. 2019, *A&A Rv*, 27, 8, doi: [10.1007/s00159-019-0119-3](https://doi.org/10.1007/s00159-019-0119-3)
- Harris, W. E. 1996, *AJ*, 112, 1487, doi: [10.1086/118116](https://doi.org/10.1086/118116)
- in't Zand, J. J. M., Hulleman, F., Markwardt, C. B., et al. 2003, *A&A*, 406, 233, doi: [10.1051/0004-6361:20030681](https://doi.org/10.1051/0004-6361:20030681)
- Ivanova, N. 2013, *Mem. Soc. Astron. Italiana*, 84, 123, doi: [10.48550/arXiv.1301.2203](https://doi.org/10.48550/arXiv.1301.2203)
- Joye, W. A., & Mandel, E. 2003, in *Astronomical Society of the Pacific Conference Series*, Vol. 295, *Astronomical Data Analysis Software and Systems XII*, ed. H. E. Payne, R. I. Jedrzejewski, & R. N. Hook, 489
- Kremer, K., Fuller, J., Piro, A. L., & Ransom, S. M. 2023, *MNRAS*, 525, L22, doi: [10.1093/mnras/525/1/22](https://doi.org/10.1093/mnras/525/1/22)
- Kremer, K., Piro, A. L., & Li, D. 2021, *ApJL*, 917, L11, doi: [10.3847/2041-8213/ac13a0](https://doi.org/10.3847/2041-8213/ac13a0)
- Kremer, K., Ye, C. S., Kiroğlu, F., et al. 2022, *ApJL*, 934, L1, doi: [10.3847/2041-8213/ac7ec4](https://doi.org/10.3847/2041-8213/ac7ec4)
- Leahy, D. A., Darbro, W., Elsner, R. F., et al. 1983, *ApJ*, 266, 160, doi: [10.1086/160766](https://doi.org/10.1086/160766)
- Lorimer, D. R., & Kramer, M. 2004, *Handbook of Pulsar Astronomy*, Vol. 4
- Lynch, R. S., Ransom, S. M., Freire, P. C. C., & Stairs, I. H. 2011, *ApJ*, 734, 89, doi: [10.1088/0004-637X/734/2/89](https://doi.org/10.1088/0004-637X/734/2/89)
- Lyne, A. G., Manchester, R. N., & D'Amico, N. 1996, *ApJL*, 460, L41, doi: [10.1086/309972](https://doi.org/10.1086/309972)
- McCarver, A. V., Maccarone, T. J., Ransom, S. M., et al. 2024, *ApJ*, 969, 30, doi: [10.3847/1538-4357/ad4461](https://doi.org/10.3847/1538-4357/ad4461)
- Minniti, D. 2018, in *Astrophysics and Space Science Proceedings*, Vol. 51, *The Vatican Observatory, Castel Gandolfo: 80th Anniversary Celebration*, ed. G. Gionti & J.-B. Kikwaya Eluo, 63, doi: [10.1007/978-3-319-67205-2\\_4](https://doi.org/10.1007/978-3-319-67205-2_4)
- Nice, D., Demorest, P., Stairs, I., et al. 2015, *Tempo: Pulsar timing data analysis*, *Astrophysics Source Code Library*, record ascl:1509.002
- Padmanabh, P. V., Ransom, S. M., Freire, P. C. C., et al. 2024, *A&A*, 686, A166, doi: [10.1051/0004-6361/202449303](https://doi.org/10.1051/0004-6361/202449303)
- Pooley, D., Lewin, W. H. G., Anderson, S. F., et al. 2003, *ApJL*, 591, L131, doi: [10.1086/377074](https://doi.org/10.1086/377074)
- Predehl, P., Hasinger, G., & Verbunt, F. 1991, *A&A*, 246, L21
- Prestage, R. M., Constantinescu, K. T., Hunter, T. R., et al. 2009, *IEEE Proceedings*, 97, 1382, doi: [10.1109/JPROC.2009.2015467](https://doi.org/10.1109/JPROC.2009.2015467)
- Price, D. C. 2016, *PyGDMS: Python interface to Global Diffuse Sky Models*, *Astrophysics Source Code Library*, record ascl:1603.013
- Price, D. C., Flynn, C., & Deller, A. 2021, *PASA*, 38, e038, doi: [10.1017/pasa.2021.33](https://doi.org/10.1017/pasa.2021.33)
- Ransom, S. 2011, *PRESTO: Pulsar Exploration and Search TOolkit*, *Astrophysics Source Code Library*, record ascl:1107.017
- Ransom, S. M., Eikenberry, S. S., & Middleditch, J. 2002, *AJ*, 124, 1788, doi: [10.1086/342285](https://doi.org/10.1086/342285)
- Ridolfi, A., Gautam, T., Freire, P. C. C., et al. 2021, *MNRAS*, 504, 1407, doi: [10.1093/mnras/stab790](https://doi.org/10.1093/mnras/stab790)
- Stappers, B., & Kramer, M. 2016, in *MeerKAT Science: On the Pathway to the SKA*, 9, doi: [10.22323/1.277.0009](https://doi.org/10.22323/1.277.0009)
- Trager, S. C., King, I. R., & Djorgovski, S. 1995, *AJ*, 109, 218, doi: [10.1086/117268](https://doi.org/10.1086/117268)
- Turk, P. J., & Lorimer, D. R. 2013, *MNRAS*, 436, 3720, doi: [10.1093/mnras/stt1850](https://doi.org/10.1093/mnras/stt1850)
- Valenti, E., Ferraro, F. R., & Origlia, L. 2007, *AJ*, 133, 1287, doi: [10.1086/511271](https://doi.org/10.1086/511271)
- van den Berg, M., Homan, J., Heinke, C. O., et al. 2024, *ApJ*, 966, 217, doi: [10.3847/1538-4357/ad2f3d](https://doi.org/10.3847/1538-4357/ad2f3d)
- Verbunt, F., & Freire, P. C. C. 2014, *A&A*, 561, A11, doi: [10.1051/0004-6361/201321177](https://doi.org/10.1051/0004-6361/201321177)
- Verbunt, F., & Hut, P. 1987, in *The Origin and Evolution of Neutron Stars*, ed. D. J. Helfand & J. H. Huang, Vol. 125, 187
- Vleeschouwer, L., Corongiu, A., Stappers, B. W., et al. 2024, *MNRAS*, 530, 1436, doi: [10.1093/mnras/stae816](https://doi.org/10.1093/mnras/stae816)
- Wu, Y., Pan, Z., Qian, L., et al. 2023, *arXiv e-prints*, arXiv:2312.06067, doi: [10.48550/arXiv.2312.06067](https://doi.org/10.48550/arXiv.2312.06067)
- Yao, J. M., Manchester, R. N., & Wang, N. 2017, *ApJ*, 835, 29, doi: [10.3847/1538-4357/835/1/29](https://doi.org/10.3847/1538-4357/835/1/29)
- Ye, C. S., Kremer, K., Ransom, S. M., & Rasio, F. A. 2024, *ApJ*, 961, 98, doi: [10.3847/1538-4357/ad089a](https://doi.org/10.3847/1538-4357/ad089a)
- Zhou, D., Wang, P., Li, D., et al. 2024, *Science China Physics, Mechanics, and Astronomy*, 67, 269512, doi: [10.1007/s11433-023-2362-x](https://doi.org/10.1007/s11433-023-2362-x)